

PAPER • OPEN ACCESS

Velocity Flow Field Characteristic on Nozzle Cavity using Central Composite Design of Computational Method for Dry Ice Blasting System

To cite this article: Mohamad Nur Hidayat Mat *et al* 2021 *J. Phys.: Conf. Ser.* **2129** 012020

View the [article online](#) for updates and enhancements.

You may also like

- [The influence of the limit stress value on the sublimation rate during the dry ice densification process](#)
J Górecki, A Fierek, K Talaka et al.
- [A physics-enabled flow restoration algorithm for sparse PIV and PTV measurements](#)
Andrey Vlasenko, Edward C C Steele and W Alex M Nimmo-Smith
- [The effect of temperature on exhaled breath condensate collection](#)
Aditya Vyas, Qi Zhang, Shyamini Gunaratne et al.



ECS The Electrochemical Society
Advancing solid state & electrochemical science & technology

242nd ECS Meeting

Oct 9 – 13, 2022 • Atlanta, GA, US

Early hotel & registration pricing ends September 12

Presenting more than 2,400 technical abstracts in 50 symposia

The meeting for industry & researchers in

BATTERIES
ENERGY TECHNOLOGY
SENSORS AND MORE!

 Register now!

 **ECS Plenary Lecture featuring M. Stanley Whittingham,**
Binghamton University
Nobel Laureate –
2019 Nobel Prize in Chemistry



Velocity Flow Field Characteristic on Nozzle Cavity using Central Composite Design of Computational Method for Dry Ice Blasting System

Mohamad Nur Hidayat Mat¹, Md Faisal Md Basir² and Mohamad Farid Sies³

¹School of Mechanical Engineering, Faculty of Engineering, Universiti Teknologi Malaysia, 81310 UTM Johor Bahru, Malaysia.

²Department of Mathematical Sciences, Faculty of Science, Universiti Teknologi Malaysia, 81310 UTM Johor Bahru, Malaysia.

³Department of Mechanical and Manufacturing, Department of Mechanical Engineering, Universiti Tun Hussein Onn Malaysia, 86400 Parit Raja, Johor, Malaysia.

Email: mn.hidayat@utm.my

Abstract. In the development of dry ice blasting nozzle geometry, the critical process parameters depend on particle jet velocity. However, very few researchers have attempted sensitivity on the velocity flow area of specific nozzle geometric parameters. A numerical simulation approach was performed in this paper using Ansys Fluent to investigate different nozzle parameters on the velocity flow field. A two-dimensional model is solved iteratively using averaged Navier-Stokes under Eulerian flow description. It was found that the velocity value increases that reach 550 m/s with an increment of the nozzle area ratio of up to 20 without influencing convergent angle and the velocity magnitude drop linearly from 525 m/s to 505 m/s in with the rise of divergent length that swell up to 700 mm and with constant convergent angle and convergent length.

1. Introduction

Industrial pollution is a massive challenge faced by a process operator due to impurities present in the system, resulting in a decrease in efficiency [1]. Due to this scenario, various removal method has been carefully design. Dry ice blasting is one of the successful removal process implemented by cleaning industries. This cleaning method characterized by non-humidity cleaning conditions and free from any secondary waste after the process compared to another conventional blasting system [2].

In addition to green environmental impact, the system is a reasonably cheap and safe cleaning method; however, one of its drawbacks directly relates to the lowest particle speed from the nozzle outlet [3]. The nozzle is a vital component of the dry ice blasting productivity. Due to this issue, many researchers began to investigate and optimize the nozzle efficiency. The subsequent finding found that the nozzle geometry influences the two-phase flow outlet and the cleaning speed [4]. From the designing process point of view, very few researchers have attempted to respond to nozzle parameters on particle velocity speed, especially using a systematic approach [5,6]. They behind this is that the study of three-dimensional model requires high computation load and longer time to achieve convergent status as the process involves high-speed compressible flow with the interaction of discrete particle model [7].

Therefore, this research employs two-dimensional model to ease computational load by using the averaged Navier–Stokes equations under Eulerian flow description. This study would consider the effect



of mass, momentum and energy exchange between the two phases [8]. Results are presented in term of response surface chart between particle velocity magnitude and nozzle geometric parameters.

2. Methodology

2.1. Geometrical Modelling

The model of nozzle geometry was created by Ansys design modeller, which directly refer to a previous literature study [6, 9]. The boundary condition and the nozzle dimension are demonstrated in Table 1 and 2, respectively. Nozzle dimension in this research consists of some parameters which are Inlet Diameter (D_i), Throat Diameter (D_t), Exit Diameter (D_e), Divergent Length (L_d), Convergent Length (L_c), and Throat Length (L_t) as shown inside Figure 1.

Table 1. Boundary Condition

Boundary Condition	Value
Inlet Pressure	600 kPa
Exit pressure (P_e)	101.33 kPa
Inlet stagnation pressure (P_o)	603.88 kPa
Inlet stagnation Temperature (T_o)	273.37 K
The temperature of Dry Ice Particle	194.50 K
Density of Dry Ice Particle	1560 kg/m ³
Heat Capacity of Dry Ice Particle	519.16 J/kg/K
Shape Factor of Dry Ice Particle	0.76

Table 2. Nozzle Dimension

Dimension	Value
Inlet diameter (D_i)	39.73 mm
Throat diameter (D_t)	10.16 mm
Exit diameter (D_e)	28.96 mm
Divergent length (L_d)	558.80 mm
Convergent length (L_c)	127 mm
Throat length (L_t)	52.83 mm

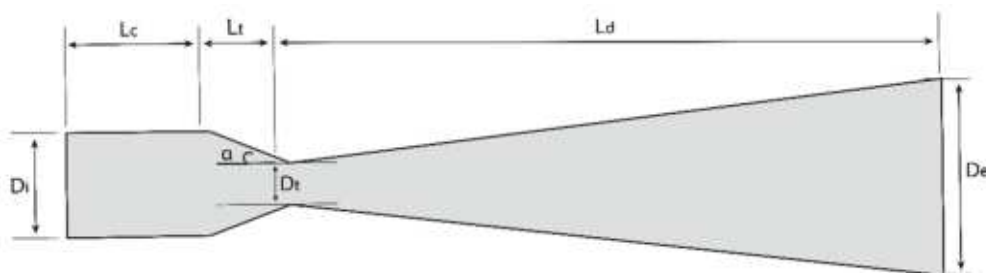


Figure 1. Nozzle dimension

2.2. Mesh of Nozzle and Central Composite Design

Computational calculation employs a finite volume method while the domain creation discretized using Ansys Mesh Modeller. The nozzle geometry consists of three major sections, namely convergent, throat and divergent section. These sections are essential for mesh refinement, especially near the throat region [10]. Throat region requires edge sizing method as the area has a narrower cross-sectional area that will cause a rapid change in velocity and pressure [11,12]. Any geometrical changes such as corner and cross-sectional area reduction need a small mesh element in which these regions have the highest changes in elemental gradient [13,14].

The domain near cylindrical and rectangular employs proximity and curvature mesh element [15,16]. The mesh quality must refer to mesh metric spectrum skewness where highest skewness gives bad accuracy in solving the solution [17]. Response surface chart plotted from variable nozzle parameters

was based on response surface methodology in which the design of the experiment utilised the central composite design approach. This method is useful for building a second order, which is a quadratic model for the response variable, without completing the three-level factorial design [18].

2.3. Governing Equation

The particle's governing equation to fluid interaction can be analysed via averaged Navier–Stokes equation under Eulerian flow description that is written in their compact Cartesian form as follows.

$$\frac{\partial \rho}{\partial t} + \frac{\partial}{\partial x_i} (\rho u_i) = 0 \quad (1)$$

$$\frac{\partial}{\partial t} (\rho u_i) + \frac{\partial}{\partial x_j} (\rho u_i u_j) = -\frac{\partial P}{\partial x_i} + \frac{\partial \tau_{ij}}{\partial x_j} \quad (2)$$

$$\frac{\partial}{\partial t} (\rho E) + \frac{\partial}{\partial x_j} (u_j (\rho E + P)) = \bar{\nabla} \cdot (\alpha_{eff} \frac{\partial T}{\partial x_i}) + \bar{\nabla} \cdot (u_j \tau_{ij}) \quad (3)$$

$$\tau_{ij} = \mu_{eff} \left(\frac{\partial u_i}{\partial x_j} + \frac{\partial u_j}{\partial x_i} \right) - \frac{2}{3} \mu_{eff} \frac{\partial u_k}{\partial x_k} \delta_{ij} \quad (4)$$

However, the turbulence models relate to the Boussinesq hypothesis in this research. Following the eddy viscosity assumption, $-\rho \overline{u'_i u'_j}$, and the average Reynolds stress tensor is proportional to the mean deformation rate tensor.

$$-\rho \overline{u'_i u'_j} = \mu_t \left(\frac{\partial u_i}{\partial x_j} + \frac{\partial u_j}{\partial x_i} \right) - \frac{2}{3} \left(\rho k + \mu_t \frac{\partial u_k}{\partial x_k} \right) \delta_{ij} \quad (5)$$

3. Results and Discussions

Figure 2 presents the response surface analysis of different nozzle geometry concerning the particle flow field at the nozzle outlet section. Figure 2a on the other hand, shows the velocity value increases that reach 550 m/s with an increment of the nozzle area ratio of up to 20 without influencing convergent angle. Besides, Figure 2b demonstrates the response of convergent angle and convergent length toward the particle velocity magnitude. The velocity flow field reaches a constant value of approximately 510 m/s for all convergent angles and length ranges. Figure 2c shows the response of convergent length and the nozzle area ratio against the velocity.

The velocity trend increases with the rise of nozzle area ratio with constant convergent length. Figure 2d highlights a response surface's result for divergent length with a convergent angle concerning velocity magnitude. The velocity magnitude drops linearly from 525 m/s to 505 m/s in with the rise of divergent length swell up to 700 mm and with constant convergent angle and convergent length, as shown in Figure 2e. Furthermore, Figure 2f presents the trend of velocity increases quadratically with a further rise of nozzle area ratio that reach maximum to around 575 m/s with nozzle area ratio and divergent lengths of 20 and 300 mm respectively.

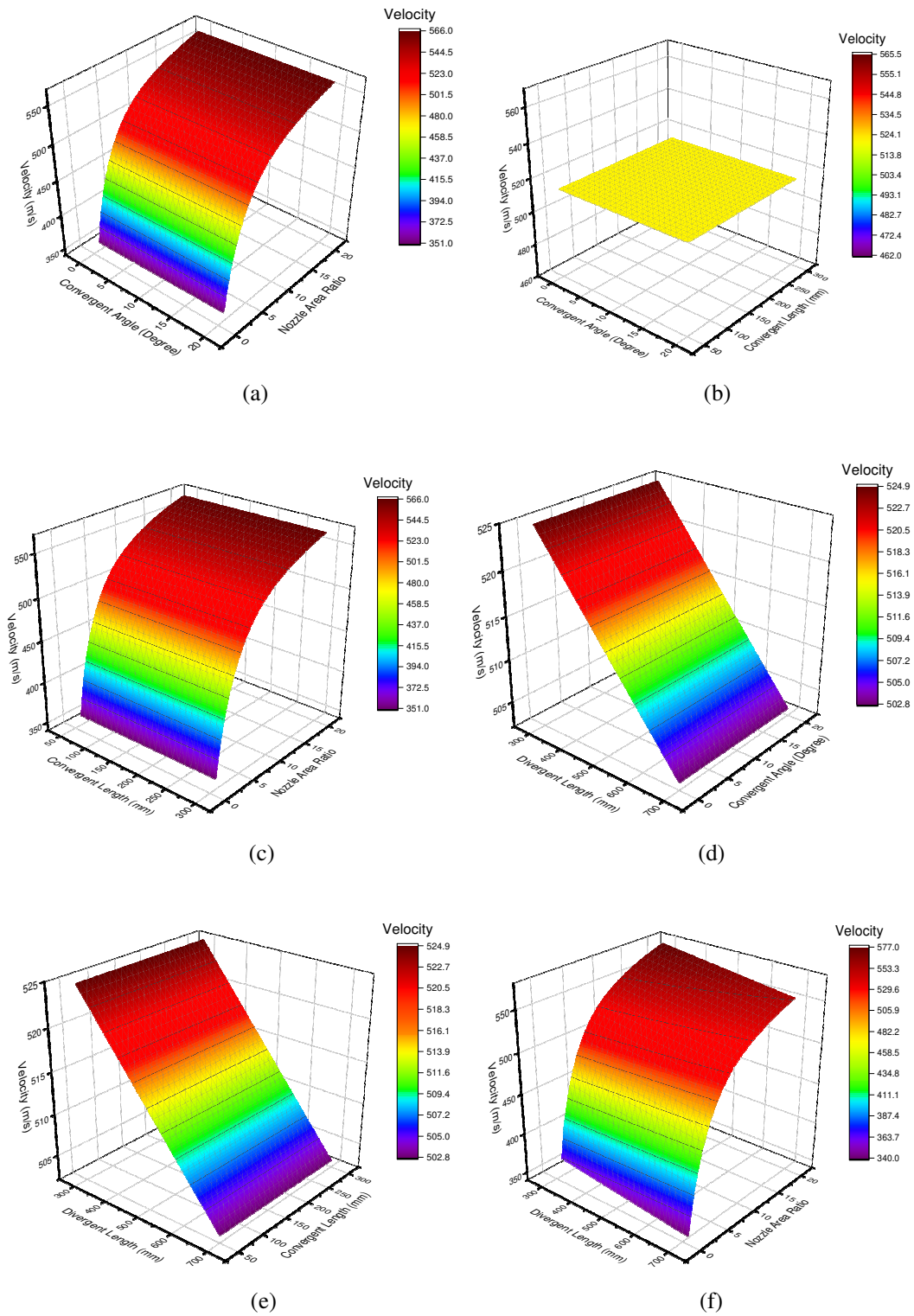


Figure 2. Response surface chart of input variable with respect to velocity magnitude

4. Conclusions

Response surface analysis using central composite design of experiment was simulated and analyzed by the steady flow of 2D single-hose dry ice blasting nozzle geometry. In the present study, a simulation has been carried out on four input variables and output parameters. Based on the simulation results, it was found that:

- Velocity value increases that reach 550 m/s with an increment of the nozzle area ratio of up to 20 without influencing the convergent angle.
- The velocity flow field reaches a constant value of approximately 510 m/s for all convergent angles and length ranges.
- The velocity magnitude drops linearly from 525 m/s to 505 m/s in with the rise of divergent length that swell up to 700 mm and with constant convergent angle and convergent length.

Apart from quantitative conclusion presented above, some future works can be extended from this research. The experimental approach can be made to solidify the result finding with supporting theoretical justification. Apart from that, a dimensional analysis could be done to determine the relationship of various nozzle geometry based on the result finding in this paper. Thus, the reader can correlate the common dimensionless parameter for standardized designing process.

References

- [1] Olajire A A 2020 *Journal of Cleaner Production*. **256** 1-21
- [2] Kohli R 2019 *Applications of Cleaning Techniques*. **11** 117-169
- [3] Melentiev R and Fang F J P T 2019 *Powder Technology*. **344** 121-132
- [4] Anyanwu I S, Hou Y, Xi F, Wang X, Yin Y, Du Q and Jiao K 2019 *International Journal of Hydrogen Energy*. **44** 13807-13819
- [5] Dzido A, Krawczyk P, and Kurkus-Gruszecka M, *Energies*. 2019. **12** 4787-4801
- [6] Dong S, Song B, Liao H L and Coddet C 2012 *Material Research Innovation*. **16** 61-66
- [7] Kloss C, Goniva C, Hager A, Amber S and Pirker S 2012 *Progress in Computational Fluid Dynamics*. **12** 140-152
- [8] Kumar N and Puranik B J A T E 2017 *Applied Thermal Engineering*. **111** 1674-1681
- [9] Hamed A, Mesalhy O, and Lehnig T 2001 *XV ISOABE Conference*. **1182** 2-7
- [10] Mat M N H, Asmuin N Z, Basir M F, Safaei M R, Kasihmuddin S M, Khairuddin T K A and Godarzi M 2020 *Journal of Thermal Analysis and Calorimetry*. **93** 1-15
- [11] Mat M N H, Asmuin N Z, Basir M F, Godarzi M, Rahman M F A, Khairulfuaad R, Jabbar B A Safaei M R and Kasihmuddin M S M 2020 *Powder Technology*. **364** 152-158.
- [12] Mat M N H and Asmuin N Z 2018 *International Journal of Integrated Engineering*. **10** 130-135
- [13] Mat M N H, Asmuin N Z, Basir M F, Goodarzi M and Hasan N H 2020 *The European Physical Journal Plus* 2020. **135** 1-11
- [14] Mat M N H, Asmuin N Z, Basir M F, Abbas T, Kasihmuddin M S M and Goodarzi M 2020 *Journal of Thermal Analysis and Calorimetry* **143** 2343-2354
- [15] Mat M N H 2019 *Tunku Tun Aminah Library UTHM*. **1** 1-150.
- [16] Mat M N H, Asmuin N Z, Hasan N H, Zakaria H, Rahman M F A, Khairulfuaad R and Jabbar B A 2019 *CFD Letters*. **11** 18-26.
- [17] Ait-Ali-Yahia D, Baruzzi G, Habashi W G, Fortin M, Dompierre J and Vallet M G 2002 *Numerical Methods in Fluids*. **39** 657-673.
- [18] Asghar A, Raman A A A, and Daud W M A W 2014 *The Scientific World Journal* **2014** 1-14

Acknowledgements: This research was supported by Ministry of Higher Education (MOHE) through Fundamental Research Grant Scheme (FRGS/1/2018/TK10/UTHM/02/15).